第37卷第1期 2021年1月
无 机 化 学 学 报 CHINESE JOURNAL OF INORGANIC CHEMISTRY
Vol.37 No.1 180-188

磁性凹凸棒土温敏性微凝胶的合成及其体外实验

李天乐[1,2] 仲 慧*[,1,2] 李小荣*[,2] 周 静[3,4] 刘易鑫[2] 胡卫成[4] 程志鹏[2] 姚 成*[,1]
([1]南京工业大学化学与分子工程学院,南京 210000)
([2]淮阴师范学院江苏低维材料化学重点实验室,淮安 223300)
([3]新疆农业大学食品科学与药学学院,乌鲁木齐 830001)
([4]淮阴师范学院生命科学学院,淮安 223300)

摘要: 通过乳液聚合法制备了叶酸(FA)接枝的磁性FA-Fe_3O_4/凹凸棒土-聚(*N*-异丙基丙烯酰胺-丙烯酰胺)(FA-Fe_3O_4/ATP-P(NIPAM-AAM))复合微凝胶(凹凸棒土=ATP,*N*-异丙基丙烯酰胺=NIPAM,丙烯酰胺=AAM),并通过X射线衍射(XRD)、振动样品磁强计(VSM)、热重(TG)、红外分析(IR)、紫外可见分光光度仪(UV)、扫描电子显微镜(SEM)和透射电子显微镜(TEM)对其进行表征。通过动态光散射(DLS)测定的低临界溶液温度(LCST)约为38.5 ℃,该温度适合于细胞实验。选择盐酸阿霉素(DOX)作为模型药物。药物负载和释放试验表明,ATP可以增加药物的负载和释放量。体外细胞毒性实验表明,与游离DOX相比,负载DOX的FA-Fe_3O_4/ATP-P(NIPAM-AAM)具有更好的生物相容性,并有望建立一个药物缓释系统。体外细胞摄取实验表明,FA-Fe_3O_4/ATP-P(NIPAM-AAM)具有靶向性,可用于靶向药物释放。

关键词: 材料化学; 磁性纳米复合材料; 乳液聚合法; 凹凸棒土; 温度响应; 靶向性;药物输送
中图分类号: O614.81 **文献标识码:** A **文章编号:** 1001-4861(2021)01-0180-09
DOI: 10.11862/CJIC.2021.017

Preparation and *in Vitro* Experiment of Attapulgite-based Microgels with Magnetic/Temperature Dual Sensitivities

LI Tian-Le[1,2] ZHONG Hui*[,1,2] LI Xiao-Rong*[,2] ZHOU Jing[3,4]
LIU Yi-Xin[2] HU Wei-Cheng[4] CHENG Zhi-Peng[2] YAO Cheng*[,1]
([1]*College of Chemistry and Molecular Engineering, Nanjing Tech University, Nanjing* 210000, *China*)
([2]*Jiangsu Key Laboratory for Chemistry of Low-Dimensional Materials, School of Chemistry & Chemical Engineering, Huaiyin Normal University, Huaian, Anhui* 223300, *China*)
([3]*College of Food Science and Pharmacy, Xinjiang Agricultural University, Urumchi* 830001, *China*)
([4]*College of Life Science, Huaiyin Normal University, Huaian, Anhui* 223300, *China*)

Abstract: The folic acid (FA)-grafted magnetic FA-Fe_3O_4/ATP-P(NIPAM-AAM) composite microgels (attapulgite=ATP, *N*-isopropyl acrylamide=NIPAM, acrylamide=AAM) were prepared via a method of emulsion copolymerization. The as-prepared microgels were characterized by X-ray diffraction (XRD), vibrating sample magnetometer (VSM), thermogravimetric analysis (TG), infrared spectroscopy (IR), UV-visible spectroscopy (UV), scanning electron microscope (SEM) and transmission electron microscope (TEM). The dynamic light scattering (DLS) results show that the low critical solution temperature (LCST) of microgel was about 38.5 ℃. The drug delivery ability of the as-prepared microgels was evaluated by using doxorubicin hydrochloride (DOX) as the model drug. Based on the drug loading and releasing results, the presence of ATP increased the amount of drug loading and releasing. Compared with free DOX, the *in vitro* cytotoxicity of DOX loaded FA-Fe_3O_4/ATP-P(NIPAM-AAM) was decreased and the

收稿日期:2020-07-08。收修改稿日期:2020-11-12。
国家自然科学基金(No.21775051,51676082,21405055)资助。
*通信联系人。E-mail:huizhong@hytc.edu.cn,lxr206206@163.com,yaocheng@njtech.edu.cn

biocompatibility was improved. Those results indicate that the microgels of FA-Fe_3O_4/ATP-P(NIPAM-AAM) can be used in potential as a slow-release drug system. The *in vitro* cellular uptake test revealed that the microgels of FA-Fe_3O_4/ATP-P(NIPAM-AAM) at the assigned site were significantly richer than that of other sites. This result indicates that the microgels of FA-Fe_3O_4/ATP-P(NIPAM-AAM) composite are targeting and expectable in the application of targeted drug releasing.

Keywords: materials chemistry; magnetic nanocomposites; emulsion polymerization; attapulgite; temperature-sensitive; targeted; drug delivery

0 Introduction

From the reports published on the International Agency for Research on Cancer (IARC), approximately 10 million new tumor cases arise and no fewer than 6 million patients die from the disease per year[1]. A main challenge in clinical treatment of tumor is how to accurately and high-efficiently deliver a nanocarrier which carries therapeutic agent to a tumor site to achieve ideal therapeutic effect. A drug delivery system is a means which enables the introduction of therapeutic drugs in the body and improves its effectiveness and safety by controlling the releasing rate, the releasing site and adjusting the releasing time. Drug delivery system is an interface between the patient and the drug[2]. In a bid to overcome *in vivo* adverse pharmacokinetic characteristics and non-specific distribution of most conventional chemotherapeutic agents, many advances in nanocarriers have been used in cancer targeted therapies[3-4].

Studies have been conducted on stimuli-responsive microgels and applied in many fields[5-8]. For their resemblance of physicochemical properties to those of the living tissues, these materials show good biocompatibilities, high water content, low interfacial tension, *etc*. *N*-isopropylacrylamide (NIPAM) is the most commonly and successfully researched materials among temperature-sensitive polymers. The lower critical solution temperature (LCST) of thermal-responsive nanogels based on NIPAM is about 32.0 ℃[9-10]. This temperature is close to that of the physiological human body. Furthermore, as the surrounding temperature increases, the structure of the polymer microgel undergoes a phase conversion from a swollen structure to collapse aggregation, which provides an opportunity for loading or releasing small molecules, potentially having expectable applications in tumor treatment[9-10]. Due to their reversible transition between dispersion and flocculation with the function of temperature, temperature variation can adjust the loading and releasing rate by PNIPAM-based nanocarriers. In addition, the LCST can adjust by adding comonomer into PNIPAM. Hydrophilic comonomer tends to increase the LCST and hydrophobic comonomer lowers the LCST, which provides an opportunity to embed or release small molecule, thus enabling drug delivery for tumor therapy[11].

In the last few years, organic and inorganic nanocomposites have become a hot spot in material science research. Attapulgite (ATP) is a hydrous magnesium-rich aluminosilicate clay mineral with chain layer structure, unique physical and chemical properties, including relatively permeability, good chemical stability and so on[12-13]. Magnetic iron oxide nanoparticles have attracted great attention in biomedical field owing to their good biocompatibility, low toxicity and high stability in physiological environment. Magnetic nanoparticles have unique characteristics and have been widely used in drug targeting and delivery for diagnosis and treatment[14]. It′s easy to separate Fe_3O_4 nanoparticles with strong paramagnetism by an external magnetic field and this property is widely used in magnetic separation and presented excellent recyclability[15-17].

Folic acid (FA) is a kind of necessary vitamin necessary for a single-carbon transfer reaction. Since FA is important for the nucleotide biosynthesis sequences, it′s consumed in large quantities through cell proliferation. Two membrane-associated proteins were used in normal cells. The former is the main approach in charge of metabolizing physiological folic acid present

in almost whole cells. Most of them are found in degenerated epithelial cells and activated macrophages. They preferentially bound and internalized oxidized folate through receptor-mediated endocytosis. Though low concentrations of the reduced folate carrier may be sufficient to meet the requirements of most normal cells, folate receptor (FR) is often overexpressed in tumor cells, which may allow malignant cells to successfully contend for the vitamin when the supply is limited[15,18].

Doxorubicin hydrochloride (DOX) has a wide range of biochemical effects in the body. It inhibits the synthesis of nucleic acids by embedding itself in DNA. This mechanism may eventually lead to the death of cancer cells and thus has anti-cancer effects. It has a significant influence on the chemotherapy of acute leukemia, lymphoma and other solid tumors. DOX is a satisfactory anticancer drug.

Herein, we synthesized FA-Fe_3O_4/ATP-P(NIPAM-AAM) based on emulsion polymerization. Due to the large surface area of ATP, the drug loading efficient is improved. The LCST of FA-Fe_3O_4/ATP-P(NIPAM-AAM) is well tuned by adjusting the composition of the two monomers before polymerization to adapt to human body temperature. Combining FA to the microgels through chemical bonds can increase the targeting ability. DOX is a model anticancer drug to carry out the *in vitro* test to verify the performance of the FA-Fe_3O_4/ATP-P(NIPAM-AAM) in identification and destruction cancer cells (Scheme 1).

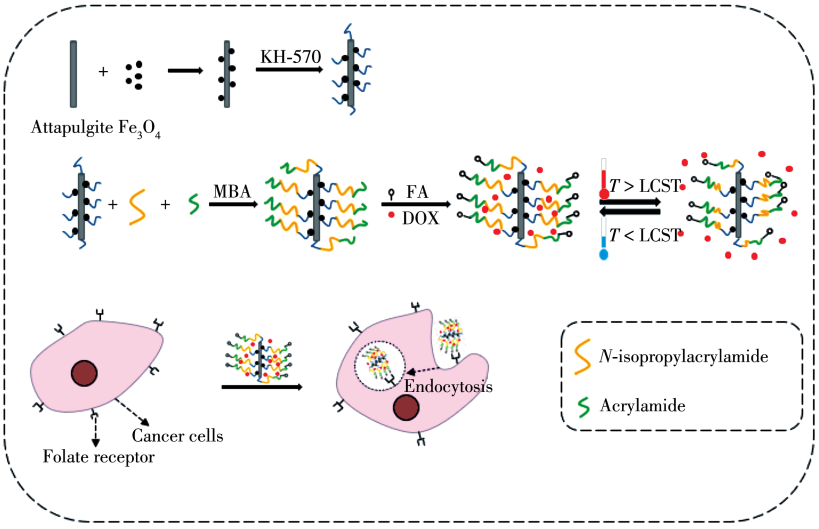

Scheme 1 Schematic diagram of synthesis and targeting process of FA-Fe_3O_4/ATP-P(NIPAM-AAM)

1 Experimental

1.1 Materials

N, *N*′-methylenebisacrylamide (MBA, 98%), *N*-isopropyl acrylamide (NIPAM, 99%), ammonium persulfate (APS, 98%) and sodium hyposulfite (SPS, 98%) were purchased from Acros Organics Co., Ltd. DMSO, toluene, ferric acetylacetonate ($Fe(C_5H_7O_2)_3$), triethylene glycol, *N*-hydroxysuccinimide (NHS, 98%), γ-methacryloxypropyl trimethoxysilane (KH-570), *N*-(3-dimethylaminopropyl)-*N*′-ethylcarbodllmidehydrochioricia (EDC, 98%), dialysis bag (M_w: 8~14 kD) and folic acid (98%) were purchased from Aladdin Chemistry Co., Ltd. (Shanghai, China). Attapulgite was purchased from Hongjin Attapulgite Instruments (Xuyi, China). Sodium dodecyl sulfate (SDS) was purchased from Alpha Chemical Industry Co., Ltd. (3-4,5-dimethylthiazol-2-yl)-2,5-diphenyltetrazolium bromide (MTT) was obtained from Sigma-Aldrich (St. Louis, MO, USA). The fetal bovine serum (FBS) was from Corning (Medford, MA, USA). Dulbecco′s modified eagle′s medium (DMEM basic), penicillin-streptomycin solution and trypsin-EDTA (0.25%) were purchased from Invitrogen-Gibco (Carlsbad, CA, USA).

1.2 Instrumentation and procedures

The morphologies and the particle size of the ob-

tained samples were characterized by transmission electron microscopy (TEM, JEOL JEM-200CX, 120 kV) and scanning electron microscopy (SEM, JEOL JSM-6700F, 10 kV). The ultraviolet-visible (UV-Vis) spectroscopy was acquired with AVATAR-360 FT-IR spectrophotometer from Nicolet Corporation. The magnetic properties of Fe_3O_4/ATP were characterized by vibrating sample magnetometer (VSM, AGFM, Iran) at 25 ℃. The crystal structure of the material was analyzed by an X-ray diffractometer with Cu *Kα* (λ =0.154 06 nm, X′pert-PRO). The tube voltage was 40 kV and the tube current was 60 mA. The scanning range was 5°~90°, and the scanning rate was 5 (°)·min^{-1}.The MTT assay was probed using a spectrophotometric plate reader (Elx808, Biotek, USA) at a wavelength of 570 nm *in vitro* uptake images and obtained by LSM700 laser confocal microscope (nikon A1). The DLS was characterized by Malvern particle size analyzer (Zetasizer Nano ZS) and the model of freeze dryer was FD-1A-50 from Beijing medical laboratory instrument Co. LTD.

1.3 Preparation of Fe_3O_4/ATP

First, 0.2 g of dried ATP and 1.000 g of Fe $(C_5H_7O_2)_3$ were mixed evenly in 30 mL of triethylene glycol under the ultrasonic condition. The mixture was heated to 270 ℃ for 2 h[19-20]. After cooling to room temperature, the prepared precipitate was washed with EtOH/deionized water for several times and dried in the vacuum oven over night at 50 ℃.

1.4 Surface modification of Fe_3O_4/ATP

Silane coupling reagent KH-570 was used as surface modifier. The vinyl group of KH-570 was introduced onto the surface of Fe_3O_4/ATP to copolymerize with NIPAM[21]. 1.0 mL of deionized water and 1.0 g of Fe_3O_4/ATP were dispersed in 100 mL of methylbenzene. Then, 3.0 mL of KH-570 was added into the mixture. In a 250 mL three-necked flask, the mixture was ultrasonificated for 40 min before stirred at 45~50 ℃ for 4 h. Finally, KH-570 modified Fe_3O_4/ATP was separated with a magnetic bar and sequentially washed with toluene, EtOH and deionized water. The KH-570-Fe_3O_4/ATP was dried at 65 ℃ in a vacuum oven.

1.5 Preparation of Fe_3O_4/ATP-P(NIPAM-AAM)

The KH-570-Fe_3O_4/ATP was dispersed into deionized water to obtain a Fe_3O_4/ATP dispersion with a concentration of 0.04 g·mL^{-1}. 0.4 g of NIPAM, the formulated amount of AAM (mass ratio of NIPAM/AAM was 1∶14), 5 mg of MBA and 2 mg of SDS were added in 2 mL of Fe_3O_4/ATP dispersion and then further diluted with 30 mL of deionized water[22-23]. After the deoxygeneration of above solution was carried out with nitrogen for 30 min, the temperature was raised to 70 ℃. 1 mL of APS (3 mg·mL^{-1}) and 1 mL of SPS (2.5 mg·mL^{-1}) were added into the solution with a syringe. The nitrogen atmosphere was maintained in the whole process. After being stirred for 6 h with a magnetic stirrer, the solution was cooled down to the room temperature and then dialyzed with the deionized water for 7 d to remove unreacted monomers and impurities to obtain Fe_3O_4/ATP-P(NIPAM-AAM). The product was frozen by a refrigerator and then stored in a freeze dryer before use.

1.6 Preparation of FA-Fe_3O_4/ATP-P(NIPAM-AAM)

First, 0.034 mmol·L^{-1} of *N*-hydroxysuccinimide (NHS), 1.3 mg of 1-ethyl-3-(3-dimethylaminopropyl) carbodiimide (EDC) and 1.3 mg of FA were dissolved in DMSO. 20 mg of Fe_3O_4/ATP-P(NIPAM-AAM) was dispersed in 20 mL of PBS (pH 7.4) and adjust the pH value to 4.5~4.7. The above FA solution was added to the Fe_3O_4/ATP-P(NIPAM-AAM) solution and stirred at room temperature for 16 h in the dark[24-25]. After adjusting the pH value to 9.0 to end the reaction, reagents were dialyzed in PBS solution (pH 7.4) and deionized water (molecular weight cutoff of 14 kD) for 6 d. The resultant FA-Fe_3O_4/ATP-P(NIPAM-AAM) was dried for the following uses.

1.7 *In vitro* study

1.7.1 *In vitro* drug loading and releasing

20 mg of Fe_3O_4/ATP-P(NIPAM-AAM) was dispersed in 20 mL of deionized water containing 5 mg of DOX. The mixture was stored in refrigerator at 4 ℃ to make the nanogel fully inflated[26-27]. The drug loading proceeded for 48 h.

The dialysis of above solution was conducted in deionized water for 4 h, whilst water was altered per half hour. The concentration of drug in outer water was

measured by UV-visible spectrophotometer, thereby the drug loading rate was calculated. DOX absorbance was measured per half hour from 26 to 50 ℃ and the temperature gradient was 2 ℃[26-27].

The DOX loading and releasing amount was determined by UV-visible spectrophotometer at the wavelength of 225 nm.

1.7.2 Cell culture

Human liver cancer cells (HepG2) were purchased from American Type Culture Collection (ATCC). HepG2 cells were cultured in DMEM medium containing 10% (*V*/*V*) FBS and 1% (*V*/*V*) antibiotics at 37 ℃ in a HERA cell 150 incubator (Thermo Fisher Scientific Inc., USA).

1.7.3 *In vitro* cytotoxicity

The MTT assay was used to determine the cytotoxicity of FA-Fe_3O_4/ATP-P(NIPAM-AAM) of HepG2 according to the previous literature[28]. Briefly, cells were seeded in 96-well plate at a density of 2×10^5 cells per well. After incubation overnight, cells were treated with different concentrations of samples. After 48 h of incubation, the medium of MTT solution was added. The cell survival rate was calculated according to the following formula:

$$\text{Cell viability}=\frac{OD_{\text{sample group}}-OD_{\text{blank group}}}{OD_{\text{negative control}}-OD_{\text{blank group}}}\times100\%$$

Where, $OD_{\text{sample group}}$ is the absorbance of sample group; $OD_{\text{negative group}}$ is the absorbance of control group; $OD_{\text{negative group}}$ is the absorbance of blank group.

1.7.4 *In vitro* cellular uptake

HepG2 cells were seeded in 96-well plates at a density of 3×10^5 cells per well and cultured incubator for an additional 16~20 h. The cells were treated with 200 μg·mL^{-1} of FA-Fe_3O_4/ATP-P(NIPAM-AAM) for indicated time points. Then the medium was removed. The cells were washed in following way: trice with PBS, fixed with 4% paraformaldehyde for 15 min, trice with PBS. Finally, cells were observed under a LSM700 laser confocal microscope after stained with an anti-fade mounting medium with DAPI.

2 Results and discussion

2.1 Qualitative characterization of Fe_3O_4/ATP

Fig. 1A shows the XRD patterns of Fe_3O_4, Fe_3O_4/ATP, and ATP. Six characteristic peaks (30.1°, 35.44°, 43.08°, 53.58°, 57.16°, and 62.78°) corresponding to the Fe_3O_4 nanoparticles (NPs) were also obtained for the Fe_3O_4/ATP, revealing that the Fe_3O_4 NPs were bonded to the ATP. What's more, the peak at 26.52° is well consistent to the primary diffraction plane of the ATP. The results indicated that the Fe_3O_4/ATP were successfully synthesized[21].

Fig. 1B exhibits the magnetic hysteresis loops of Fe_3O_4 and Fe_3O_4/ATP obtained with the VSM for magnetic fields from −5 to 5 kOe. The maximum values of magnetization saturation of the Fe_3O_4 and Fe_3O_4/ATP were 9.73 and 6.16 emu·g^{-1}. Compared with Fe_3O_4, the saturation magnetization of Fe_3O_4/ATP was reduced. The difference in saturation magnetization was attributed to the non-magnetic ATP clay particles[21].

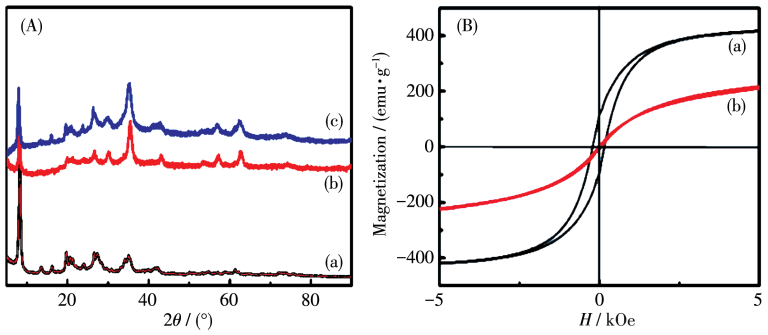

Fig.1 (A) XRD patterns of (a) ATP, (b) Fe_3O_4 and (c) Fe_3O_4/ATP; (B) VSM patterns of (a) Fe_3O_4 and (b) Fe_3O_4/ATP

2.2 Morphology characterization of FA-Fe_3O_4/ATP-P(NIPAM-AAM)

The TEM images depicted in Fig. 2a and 2b show the morphology and structure of Fe_3O_4/ATP and FA-Fe_3O_4/ATP-P(NIPAM-AAM). It is found that there is a gray layer on the edge of Fe_3O_4/ATP. This result indi-

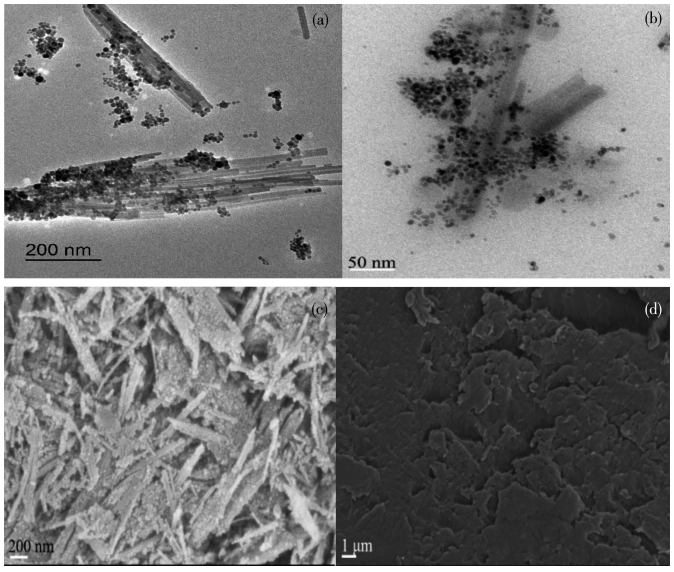

Fig.2　TEM images of (a) Fe_3O_4/ATP and (b) Fe_3O_4/ATP-P(NIPAM-AAM); SEM images of (c) Fe_3O_4/ATP and (d) Fe_3O_4/ATP-P(NIPAM-AAM)

cates that the coating of temperature responsive polymer on the Fe_3O_4/ATP is successful.

The surface morphology of the Fe_3O_4/ATP and FA-Fe_3O_4/ATP-P(NIPAM-AAM) was probed by SEM. Fig. 2c and 2d are the SEM images of the Fe_3O_4/ATP and FA-Fe_3O_4/ATP-P(NIPAM-AAM) respectively. As a result, the irregular surface of Fe_3O_4/ATP implies that a layer of P(NIPAM-AAM) gel was coated on the surface of FA-Fe_3O_4/ATP particles.

2.3　Qualitative characterization of FA-Fe_3O_4/ATP-P(NIPAM-AAM)

Fig. 3A presents the IR spectra of ATP, Fe_3O_4, Fe_3O_4/ATP, KH-570-Fe_3O_4/ATP, P(NIPAM-AAM) and Fe_3O_4/ATP-P(NIPAM-AAM), respectively. The curve of ATP shows an apparent peak at 1 035 cm^{-1}, corresponding to the stretching vibration peak of Si—O of attapulgite clay. The stretching vibration peak observed in the curve of Fe_3O_4 was at 580 cm^{-1} according to the Fe—O of Fe_3O_4. The curve c in Fig.3A presents the characteristic absorption peaks of Fe_3O_4 and ATP. Compared with Fe_3O_4/ATP, the stretching vibration peaks of —CH_3 and —CH_2 appeared in the curve of KH-570-Fe_3O_4/ATP, which are at about 2 876 and 2 930 cm^{-1}, indicating the successful modification of KH-570. For P(NIPAM-AAM), the peak at 1 385 and 1 456 cm^{-1} are C—H stretching vibration peaks on isopropyl, 1 547 cm^{-1} is the bending vibration peak of —NH, and 2 876, 2 930 and 2 973 cm^{-1} are the stretching vibration peaks of —CH_3 and —CH_2, 1 644 cm^{-1} is the stretching vibration peak of the C═O double bond. 1 035 cm^{-1} is the bending vibration peak of Si—O. Compared with P(NIPAM-AAM), there are characteristic absorption peaks of Si-O and Fe-O for Fe_3O_4/ATP-P(NIPAM-AAM), indicating the successful grafting of Fe_3O_4/ATP-P(NIPAM-AAM)[19].

Fig. 3B shows the TG curves of ATP, Fe_3O_4/ATP, KH-570-Fe_3O_4/ATP and Fe_3O_4/ATP-P(NIPAM-AAM). From the picture, we can see that compared to KH-570/Fe_3O_4/ATP, the weight loss of Fe_3O_4/ATP-P(NIPAM-AAM) increased, indicating that P(NIPAM-AAM) has been coated onto KH-570-Fe_3O_4/ATP successfully.

Fig. 3C shows the UV-Vis spectra of FA, Fe_3O_4/ATP-P(NIPAM-AAM) and FA-Fe_3O_4/ATP-P(NIPAM-AAM). The absorption peak of FA was 225 nm and the absorption peak of Fe_3O_4/ATP-P(NIPAM-AAM) was 280 nm. From the above results, the FA-Fe_3O_4/ATP-P (NIPAM-AAM) was synthesized successfully.

As shown in Fig. 3D, the thermo-sensitive profile of FA-Fe_3O_4/ATP-P(NIPAM-AAM) was characterized in the temperature range of 27.0~49.0 ℃ by DLS monitoring hydrodynamic diameter (D_h). It is clear that compared with the LCST (32.0 ℃) of PNIPAM microgel, the LCST of FA-Fe_3O_4/ATP-P(NIPAM-AAM) was around 38.5 ℃ due to the hydrophilic group of acryl-

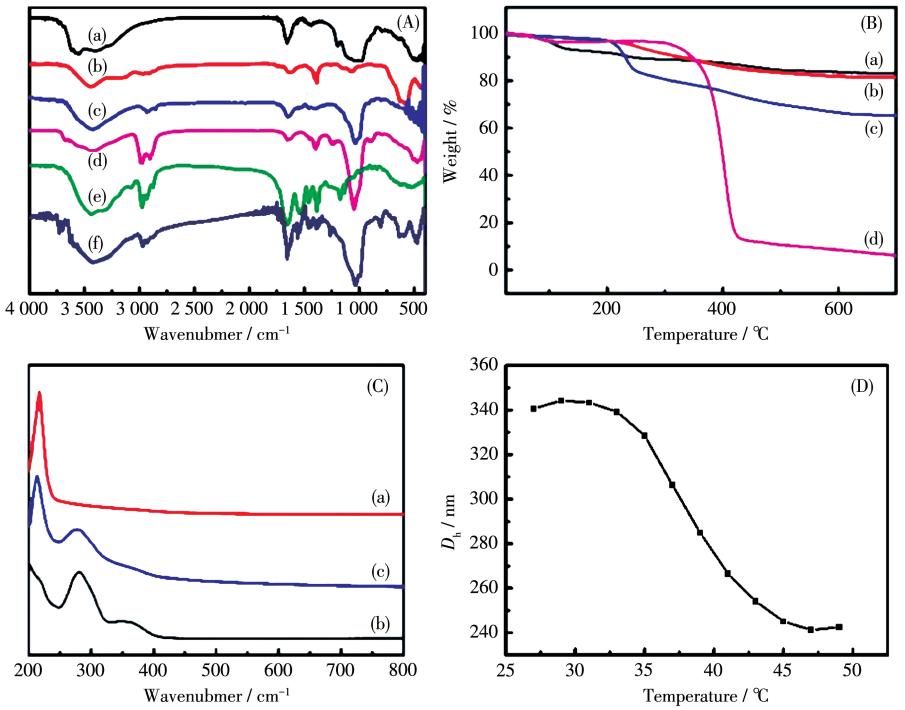

Fig.3 (A) IR spectra of (a) ATP, (b) Fe_3O_4, (c) Fe_3O_4/ATP, (d) KH-570-Fe_3O_4/ATP, (e) P(NIPAM-AAM) amd (f) Fe_3O_4/ATP-P(NIPAM-AAM); (B) TG curves of (a) ATP, (b)Fe_3O_4/ATP, (c) KH-570-Fe_3O_4/ATP and (d) Fe_3O_4/ATP-P(NIPAM-AAM); (C) UV-Vis spectra of (a) FA, (b) Fe_3O_4/ATP-P(NIPAM-AAM) and (c) FA-Fe_3O_4/ATP-P(NIPAM-AAM); (D) DLS curve of FA-Fe_3O_4/ATP-P(NIPAM-AAM)

amide. The temperature is close to that of human body and it's expected to be applied to the study of targeted sustained release cancer drugs.

2.4 *In vitro* assay

2.4.1 *In vitro* drug loading and releasing

Fig.4 exhibits the DOX releasing amount spectra of P(NIPAM-AAM) and Fe_3O_4/ATP-P(NIPAM-AAM) from 26.0 to 28.0 ℃. In Fig4a, the increase of releasing amount of DOX was obvious. It may be ascribed to the free DOX which was unloaded on P(NIPAM-AAM) microgel. The shape of P(NIPAM-AAM) and Fe_3O_4/ATP-P(NIPAM-AAM) curves was similar between 26.0~30.0 ℃, namely two-stage releases. There was a sharp hopping on curve of Fe_3O_4/ATP-P(NIPAM-AAM) at around 38.5 ℃ due to the swell-shrink of nanogel corresponding to the analysis of DLS. Compared with P(NIPAM-AAM), the loading efficiency of Fe_3O_4/ATP-P(NIPAM-AAM) rose from 62% to 79% and the releasing efficiency increased from 36% to 56%. The advantage of ATP is apparent to raise the adsorption capacity and the releasing amount.

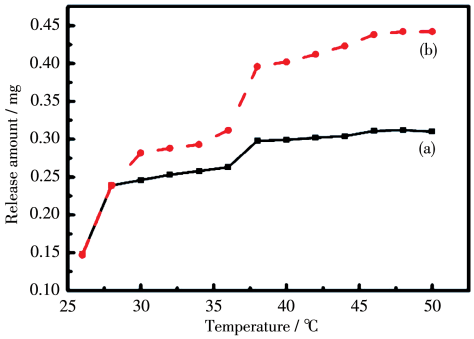

Fig.4 Plots of releasing amount of (a) P(NIPAM-AAM) and (b) Fe_3O_4/ATP-P(NIPAM-AAM)

2.4.2 *In vitro* cytotoxicity

To evaluate the safety of FA-Fe_3O_4/ATP-P(NIPAM-AAM), HepG2 cells were treated with 0, 6.25, 12.5, 25, 50, and 100 μg·mL^{-1} DOX, 0, 31.65, 63.29, 126.58, 253.16, and 506.32 μg·mL^{-1} FA-Fe_3O_4/ATP-P(NIPAM-AAM) and 0, 25.4, 50.79, 101.58, 203.16, and 406.32 μg·mL^{-1} DOX loaded FA-Fe_3O_4/ATP-P(NIPAM-AAM), respectively. MTT was used to detect cell viability. As shown in Fig.5a, after treatment with different concentrations of FA-Fe_3O_4/ATP-P(NIPAM-

AAM) for 48 h, no significant cytotoxicity was observed on HepG2 cells. The cell viability was above 1.0, indicating that FA-Fe_3O_4/ATP-P(NIPAM-AAM) promoted the growth, rather than inhibited, the cell viability. The result indicates that the synthesized FA-Fe_3O_4/ATP-P(NIPAM-AAM) polymer is safe and can be utilized as a media for drug delivery in biomedical field.

From Fig.5b and 5c, a dose-dependent inhibitory effect of DOX and DOX loaded FA-Fe_3O_4/ATP-P(NIPAM-AAM) was observed on HepG2 cells. The cytotoxicity increased as the concentration increased. However, the cytotoxicity of free DOX was weaker than that of DOX loaded FA-Fe_3O_4/ATP-P(NIPAM-AAM). This is mainly attributed to the targeting ability of FA. The IC_{50} (the concentration at which cell proliferation is half inhibited) values of free DOX and DOX loaded FA-Fe_3O_4/ATP-P(NIPAM-AAM) were 46 and 19 μg·mL^{-1} respectively. The inhibitory effect on cancer cells of DOX loaded FA-Fe_3O_4/ATP-P(NIPAM-AAM) was stronger than that of free DOX.

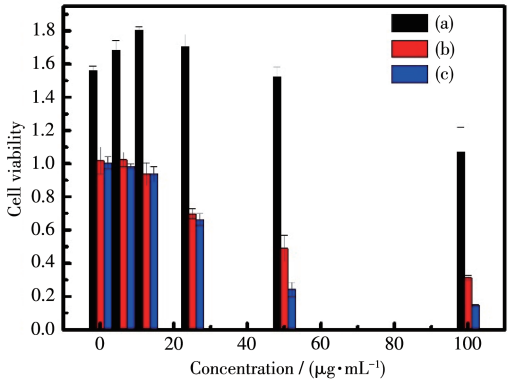

Fig.5　MTT test of (a) FA-Fe_3O_4/ATP-P(NIPAM-AAM), (b) free DOX and (c) DOX loaded FA-Fe_3O_4/ATP-P(NIPAM-AAM)

2.4.3　*In vitro* cellular uptake

For further research on the *in vitro* targeting of liver cancer cells by FA-Fe_3O_4/ATP-P(NIPAM-AAM), DOX was chosen as model drugs to identify the cellular uptake of microgels. A qualitative test of cellular uptake was performed using confocal laser scanning microscope (CLSM) of HepG2 cells after 3 or 6 h of exposure. It should be noted that the blue fluorescent signal was the nucleus of DAPI negative staining and the surrounding red fluorescent signal was the intake of DOX. As shown in Fig.6, DOX loaded FA-Fe_3O_4/ATP-P

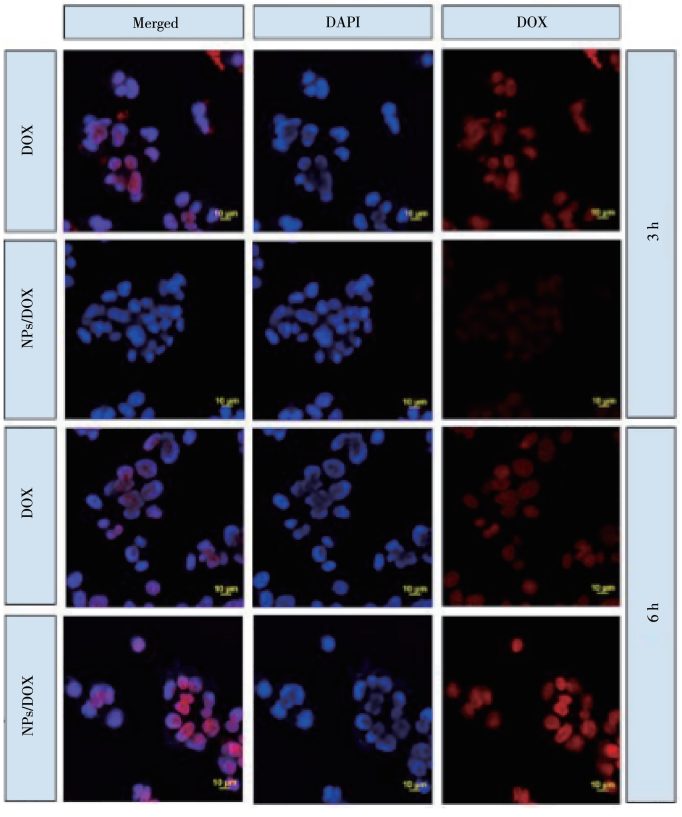

Fig.6　*In vitro* cellular uptake assay of free DOX and DOX loaded FA-Fe_3O_4/ATP-P(NIPAM-AAM) (NPs/DOX)

(NIPAM-AAM) was swallowed intracellularly by HepG2 cells after incubating HepG2 cells with DOX loaded FA-Fe_3O_4/ATP-P(NIPAM-AAM) for 3 h. A red fluorescent signal was observed arising from the cytoplasmic matrix. CLSM test′s results showed that when the time is prolonged to 6 h, the red fluorescent signal in the cells of the free DOX group was almost unchanged when compared with the HepG2 cells incubated for 3 h. In contrast, the red fluorescent signal of FA-Fe_3O_4/ATP-P(NIPAM-AAM)-DOX was significantly enhanced relative to the group incubated for 6 h. It can verify its targeting ability.

3 Conclusions

In summary, magnetic and temperature-sensitive nanoparticle microgels FA-Fe_3O_4/ATP-P(NIPAM-AAM) with targeting were synthesized by emulsion polymerization method. The phase transition temperature rose from 32.0 to 38.5 ℃, which is slightly higher than that of human body and suitable for cell experiment *in vitro*. *In vitro* cell test results show that the FA-Fe_3O_4/ATP-P(NIPAM-AAM) exhibits good biocompatibility. At the same time, the microgels with targeting ability can effectively prolong the time of drug release and action. *In vitro* drug release experiments show that ATP can increase drug loading and drug release. This material is expected to accurately release anticancer drugs to tumor cells so as to reduce side effects, which is expanding the application of targeted tumor therapy.

References:

[1] Iyer A. K, Singh A, Ganta S, Amiji M M. *Adv. Drug Delivery Rev.*, **2013**,**65**(13/14):1784-1802

[2] Jain K K. *Methods Mol. Biol.*, **2008**,**437**:1-50

[3] Peng J, Zhang W L, Ai S L, Zhang Y H, Liu J Y, Liu J, He P X, Li Y. *Nanotechnology*, **2019**,**30**(11):115701

[4] Li R, Nie W, Yang W. *Mater. Res. Express*, **2019**,**6**(7):075048

[5] Hopkins S, Carter S. R, Haycock J W, Fullwood N J, MacNeil S, Rimmer S. *Soft Matter*, **2009**,**5**(19):3701-3712

[6] Matsune H, Ono T, Yoshida R, Yamamoto T, Kishida M. *Chem. Lett.*, **2019**,**48**:1058-1060

[7] Sakai K, Sawa M, Nomura K, Endo T, Tsuchiya K, Sakamoto K. *Chem. Lett.*, **2016**,**45**:655-657

[8] Motiei M, Dreifuss T, Sadan T, Omer N, Blumenfeld-Katzir T, Fragogeorgi E. *Chem. Lett.*, **2019**,**48**:291-294

[9] Chen S J, Zhang Q Y, Gu J W, Ma M L, Zhang L, Zhou J, Zhou Y Y. *Colloid. Polym. Sci.*, **2015**,**290**(12):1207-1213

[10]Xu G. Wu W T, Wang Y, Pang W, Lu F. *Nanotechnology*, **2006**,**17**(10):2458-2465

[11]Zhang K J, Zhou D, Wang Z G, Zhang Y H, He P X. *Nanotechnology*, **2019**,**30**(35):355604

[12]Li X M, Zhong H, Li X R, Jia F F, Cheng Z P, Zhang L L, Yin J Z, An L T, Guo L P. *Mater. Sci. Eng. C*, **2014**,**45**:170-175

[13]Han Y, Chen H F, Chen D J. *J. Mater. Sci.*, **2010**,**45**(9):2372-2380

[14]Wang D, Duan H, Lu J H, Lv C. *J. Mater. Chem. A*, **2017**,**5**(10):5088-5097

[15]Lu Y J, Low P S. *Adv. Drug Deliver. Rev.*, **2012**,**54**(5):342-352

[16]Sahoo S L, Liu C H, Wu W C. *RSC Adv.*, **2017**,**7**:22468-22478

[17]Dutta B, Nema A, Shetake N G, Gupta J, Hassan P A. *Mater. Sci. Eng. C*, **2020**,**112**:110915

[18]Yang P, Zeng H, Liu J. *J. Mater. Chem. B*, **2013**,**1**(39):5298-5308

[19]Fu M, Zhang Z P. *Mater. Lett.*, **2018**,**226**:43-46

[20]Kim Y H, Sim B, Choi H J. *Colloids Surf. A*, **2016**,**507**:103-109

[21]Zhao Y J, Chen Y, Li M S, Zhou S Y, Xue A L, Xing W H. *J. Hazard Mater.*, **2009**,**171**(1/2/3):640-646

[22]Wang C N, Wang Y Y, Jin Y L, Xu T, Yuan L, Fang J H. *J. Nanosci. Nanotechnol.*, **2015**,**15**(9):6784-6789

[23]Han H D, Shin B C, Choi H S. *Eur. J. Pharm. Biopharm.*, **2006**,**62**(1):110-116

[24]Jo A, Lim D, Kim H. S*ci. Rep.*, **2017**,**7**:41090

[25]Ma C B, Shi Y, Pena D A, Peng L L, Yu G H. *Angew. Chem.*, **2015**, **127**(25):7484-7488

[26]Chen Y, Chen Y B, Nan J Y, Wang C, Chu F. *J. Appl. Polym. Sci.*, **2012**,**124**(6):4678-4685

[27]Li A H, Ma H J, Feng S Y, Liu J. *RSC Adv.*, **2016**,**6**(39):33138-33147

[28]Zhang J, Jiang Y, Li Y, Li W, Hu W. *Carbohydr. Polym.*, **2019**,**230**:115576